Spectroscopic Investigation of the Electronic $\tilde{A}^1A''-\tilde{X}^1A'$ Transition of HSiNC

Corey J. Evans* and Matthew R. Dover

Department of Chemistry, University of Leicester, University Road, Leicester, LE1 7RH, United Kingdom

Received: April 1, 2009; Revised Manuscript Received: June 8, 2009

The first spectroscopic investigation of the $\tilde{A}^1A''-\tilde{X}^1A'$ transition of HSiNC has been reported. The $\mathbf{0_0^0}$ band of the $\tilde{A}^1A''-\tilde{X}^1A'$ transition has been rotational resolved using laser-induced fluorescence spectroscopy, and ground- and excited-state rotational and centrifugal distortion constants were evaluated. Ten additional vibrational bands belonging to HSiNC have also been observed in the laser-induced fluorescence spectrum and have been assigned based on predicted anharmonic vibrational frequencies. Because of the large change in geometry upon excitation, a number of axis-rotation peaks have been observed in the $\mathbf{0_0^0}$ band, and the axis-rotation angle (θ_T) has been estimated to be $1.0 \pm 0.2°$. Dispersed fluorescence spectroscopy has also been carried out, and a number of overtones of the ν_3 fundamental (Si−H wagging mode) have been observed in the ground state, and its anharmonic parameter (x_e) was evaluated.

Introduction

The first electronic spectroscopic study on the halosilylenes was conducted many years ago. In this work the spectra of HSiCl and HSiBr were first recorded from the flash photolysis of SiH_3Cl and SiH_3Br at room temperature.[1] The authors were able to rotationally resolve fine structure but were unable to assign asymmetry splittings at low K due to congestion in the spectra. The most interesting feature of the spectra of HSiCl and HSiBr was the occurrence of "forbidden" $\Delta K_a = 0$ and ± 2 sub-bands. The authors of the paper assessed these anomalies and suggested that they were caused by a triplet−singlet transition, although there were no apparent spin splittings detected in the spectra.

Another possible reasoning for these sub-bands, added as a note in the proof of the original study by Herzberg and Verma, was that the anomalies were a result of axis rotation (axis-switching). This was assumed not to be the case, as the preliminary calculations carried out indicated that the appearance of these sub-bands would not be as intense as those observed in the spectrum. Subsequent work by Hougen and Watson showed that axis-rotation was in fact the most likely reason for these anomalous sub-bands.[2] Later, reinvestigations of HSiCl and HSiBr were carried out by the Clouthier group using high-resolution laser-induced fluorescence (LIF) spectroscopy and supersonic jet techniques allowing better resolved spectra of both species to be obtained.[3,4] As a result, the Clouthier group were able to further confirm the identity of the spectral carriers and conclusively identify the peaks attributed to axis-rotation, as there was no evidence of spin splittings. Work on HSiF and HSiI have also been carried out and they also show the effects of axis-rotation.[5−7]

Over the last two decades a number of research groups have carried out theoretical and experimental studies to obtain spectroscopic parameters to aid in the detection of new silicon containing species. One of these investigations lead to two new species, HSiCN and HSiNC, being spectroscopically observed in the laboratory.[8] Both of these species were regarded as being very strong candidates for detection in the interstellar medium due to fact that similar species have already been observed in space (e.g., SiCN).[9] In this work, Sanz et al. used a high-voltage electric discharge source coupled to a molecular beam Fourier transform microwave spectrometer to study both HSiCN and HSiNC and to obtain rotational constants for a number of different isotopomers of each species allowing the elucidation of their structures. They found that both HSiCN (cyanosilylene) and HSiNC (isocyanosilylene), like the analogous halosilylenes, are bent molecules with C_s symmetry, with the H−Si−X (X = C or N) angle being ∼95°. The spectra also indicated that there was very little observed difference in the intensity profiles of the spectra recorded for each species and there was no indication, other than the citation of previous computational studies, as to which of the two species was more stable.

In the first of these computational studies, Flores et al. carried out high-level calculations on the six lowest-lying singlet isomers as well as their corresponding triplet states at the B3LYP/6-311(d, p) level of theory.[10] In all cases it was found that the triplet isomers were considerably higher in energy. The two lowest lying singlet isomers were found to be HSiCN and HSiNC (lying 9.2 kJ mol^{-1} higher in energy than HSiCN), and in both cases the symmetry of the ground electronic state was determined to be $^1A'$ with the H−Si−X (X = C or N) angle determined to be ∼95°, which agreed well with the experimental results.[8] Furthermore, Flores et al. carried out calculations on the vertical excitation of each isomer to the lowest $^1A''$ electronic state, providing vertical excitation energies by means of multiconfiguration self-consistent field (MCSCF) and multireference configuration interaction (MRCI) calculations. For HSiCN and HSiNC, the determined vertical excitation energies were 2.55 eV (20567 cm^{-1}) and 2.72 eV (21938 cm^{-1}), respectively.

In the more recent theoretical study by Wang et al. the potential energy surfaces of the neutral, cationic, and anionic isomers of the [H, Si, C, N] system were determined at the B3LYP/6-311(d) level of theory.[11] Like the work by Flores et al., they found that the lowest two isomers were HSiCN and HSiNC, with HSiCN being 10.0 kJ mol^{-1} more stable than HSiNC.

Prior to work by Sanz et al., a matrix study by Maier et al. generated HSiCN and HSiNC from the co-condensation of

* To whom correspondence should be addressed. E-mail: cje8@le.ac.uk. Phone: +44 116 252 3985. Fax: +44 116 252 3789.

10.1021/jp902966y CCC: $40.75
Published on Web 07/02/2009

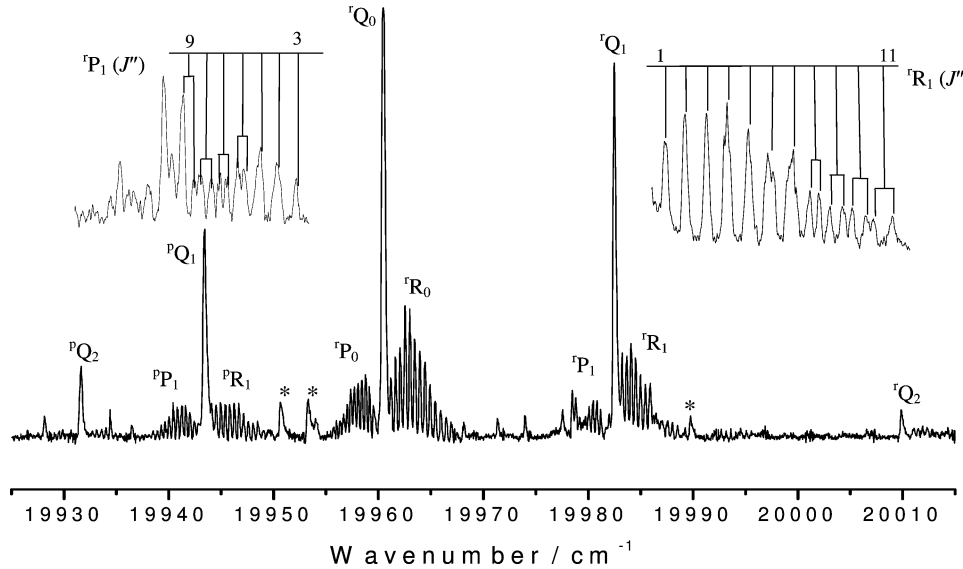

Figure 1. The medium resolution spectrum of the 0_0^0 band of HSiNC showing some of the rotational branch assignments. The asterisks mark the axis-rotation peaks. The inserts in the upper left and right corners shows the resolved asymmetry splittings in the $^rP_1$ and $^rR_1$ branches, respectively. The rotational temperature of the spectrum is estimated to be 15 K.

thermally generated silicon atoms with hydrogen cyanide in an argon matrix. The resulting matrix was investigated using IR, and a number of vibrational bands were attributed to HSiCN and HSiNC after comparisons with vibrational frequencies calculated at the B3LYP/6-311G(d,p) level of theory.[12] Like the previous studies, the HSiCN isomer was predicted to be the lowest lying isomer.

In this work we shall present the first spectroscopic investigation of the $\tilde{A}^1A''-\tilde{X}^1A'$ transition of HSiNC using LIF spectroscopy and evaluate the rotational constants in the ground state and the first $^1A''$ excited electronic state. Analysis of the vibrational modes in both states will also be discussed.

Experimental Procedure

A room temperature sample of trimethylsilylcyanide ($(CH_3)_3SiCN$, Acros Chemicals, 98%; used without further purification) was placed in a glass bubbler, and a stream of argon passed through the sample at a pressure of 2 bar to allow the vapor to mix. This gas flow was then expanded through a pulsed valve (General Valve, Series 9) into a 3 mm flow channel drilled through a 26 mm long Delrin cylinder ($d = 50$ mm) attached to the end of the pulsed valve. Inside the Delrin cylinder were two stainless steel ring electrodes separated by a 1 mm PTFE spacer positioned such that the discharge occurs along the flow channel. The high-voltage discharge design is similar to that used by Clouthier group.[13] At the appropriate time delay after the pulsed valve has fired, a high-voltage (2−6 kV) pulse of $\approx 4\ \mu$s duration was applied to one of the electrodes via a Tesla coil, while the other was grounded. The electric discharge efficiently dissociated the pseudohalosilane precursor into readily detectable amounts of HSiNC. The pulsed discharge apparatus was mounted near the center of a vacuum chamber pumped by a large turbo molecular pump, backed by a roots blower and rotary pump.

Low (0.50 cm^{-1}) and medium (0.10 cm^{-1}) resolution LIF spectra were recorded using a 355 nm pumped tunable pulsed dye laser (Quanta-Ray PDL-3). The laser beam crossed the supersonic expansion approximately 50 mm downstream from the discharge source. The resulting fluorescence was imaged through an appropriate cutoff filter, at right angles to the jet, onto the photocathode of a photomultiplier tube (Electron Tubes, B2F/RFI). To gain maximum light collection, an aluminum coated concave spherical mirror was mounted inside the vacuum chamber directly opposite the fluorescence collection optics. All spectra were calibrated with lines from a neon-filled hollow cathode lamp and simultaneously recorded etalon fringes (FSR 1.0 cm^{-1}). The LIF spectra and calibration signals were digitized on an oscilloscope and captured by a PC using software written in LabView.

Dispersed fluorescence (DF) spectra were obtained by fixing the wavelength of the dye laser to the $^pQ_1$ branch of a vibrational band in the LIF spectrum and imaging the resultant fluorescence onto the entrance slit of a 0.5 m scanning monochromator (Acton Research SpectraPro 2500i) fitted with a 1800 lines/mm grating

TABLE 1: Ground-State Rotational Constants (in cm^{-1}) of HSiNC and HSiCN

constants	this work[a] HSiNC	ab initio[b] HSiNC	microwave[c] HSiNC	ab initio[b] HSiCN	microwave[c] HSiCN
A	7.5713(99)	7.4353	7.555(91)	7.5385	8.171(22)
B	0.207139100[d]	0.2023	0.207139100(15)	0.1758	0.179117066(18)
C	0.201351247[d]	0.1969	0.201351247(16)	0.1718	0.174803436(18)
$D_J \times 10^8$	9.07[d]		9.07(13)		7.46(18)
$D_{JK} \times 10^6$	1.769[d]		1.769(19)		4.076(25)
D_K	0.0351(21)				
std dev[c]	0.022[e]				
no. lines	116		26		30

[a] Numbers in parentheses are 1σ uncertainties in units of the last significant digit. [b] This work. Calculated at the MP2 level of theory using the aug-cc-pVTZ basis set [c] From ref 8. [d] Fixed to ref 8 value. [e] rms of fit (in cm^{-1}).

blazed at 500 nm. The wavelength resolved fluorescence signals were detected with a Peltier cooled charge-coupled device camera (PI-MAX system) and processed using the WinSpec32 software supplied with the instrument. The monochromator was calibrated to an estimated accuracy of $\pm$ 2 cm^{-1} using known emission lines from a mercury lamp.

Computational Methods

As discussed above, there has already been some theoretical work carried out on the isomers of the [H, Si, C, N] system. To aid in the assignment of experimental data, in particular that of the excited state, additional calculations were carried out using the Gaussian03 program package.[14] The geometries of the [H, Si, C, N] isomers were fully optimized at different levels of theory using the augmented triple-ζ correlated consistent basis set (aug-cc-pVTZ) of Dunning et al.[15−17] The methods used include, the hybrid density functional method B3LYP,[18] the second order Møller−Plesset (MP2)[19−21] method using the frozen core technique, and the quadratic configuration interaction method including singles and doubles, QCISD.[22] Further single-point calculations were carried out using QCISD(T), using the QCISD structure to obtain more accurate energies. Finally, to obtain accurate values for transition energies the symmetry adapted cluster-configuration interaction (SAC−CI) method of Nakatsuji et al. was implemented.[23] First "level-two" calculations were carried out to optimise the structure, followed by further single-point calculations at "level three" to obtain the energies. For each species vibrational frequencies were evaluated at the optimized geometry.

Results

Preliminary low resolution scans using the precursor trimethylsilylcyanide showed a series of vibrational bands ranging between 19950 and 25000 cm^{-1}; it was thought the observed bands were from the $\tilde{A}^1A''-\tilde{X}^1A'$ transition of either HSiCN or HSiNC or both, as the spectral features of the vibrational bands closely resembled HSiF and HSiCl.[4,7] The band at $\sim$19950 cm^{-1} was considered to be the 0_0^0 band, and a medium resolution scan was recorded, and a rotational analysis was carried out. Since microwave studies on both HSiCN and HSiNC have previously been carried out, accurate rotational constants are available for these species allowing identification of the carrier of the signal.[8]

Rotational Analysis

In the medium resolution spectra of the 0_0^0 band the Q-branches of each sub-band could not be rotationally resolved, so the analysis relied only on the rotational structure of the P and R branches of each sub-band. Figure 1 shows a portion of the medium resolution scan of the 0_0^0 band, where the asymmetry splittings of the $^rR_1$ sub-band are partially resolved.

The assignment of the 0_0^0 band was straightforward. The 0_0^0 band is a C-type band, and the assigned lines were fitted using Watson's S-reduced Hamiltonian[24] with I^r representation in the spectral fitting program SPFIT.[25] Transitions with $K_a'' = 0$, 1, and 2 were assigned with J'' values up to 14 for the strongest branches. In the final fit the ground state values of the rotational constants B and C were also fixed to the microwave values, while D_J and D_{JK} for both states were fixed to the microwave values. Unfortunately, due to the lack of observed sub-bands, it was only possible to determine D_K for the ground state. For the excited state D_K was fixed to zero. The ground state value of D_K is quite large (0.0351 cm^{-1}); however, it compares well with the values obtained for the halosilylenes.[3−5,7]

TABLE 2: Excited-State Rotational Constants (in cm^{-1}) of the 0_0^0 Band of the $\tilde{A}^1A''-\tilde{X}^1A'$ Transition of HSiNC

constants	0_0^0 (this work)	ab initio[a]	ab initio
A	9.99616(99)	10.23	9.840[b]
B	0.20956(13)	0.2047	0.2048[b]
C	0.20509(20)	0.2007	0.2006[b]
$D_J \times 10^8$	9.07[c]		
$D_{JK} \times 10^6$	1.769[c]		
T_0	19950.5802(62)	15850	19820[d]
std dev[e]	0.022		
no. lines	116		

[a] This work. Caclulated at the MP2 level of theory using the aug-cc-pVTZ basis set. [b] This work. Calculated at the SAC−CI level of theory using the aug-cc-pVDZ basis set. [c] Fixed to ground state values. [d] This work. Calculated at the SAC−CI level of theory using the aug-cc-pVTZ basis set (geometry fixed to the aug-cc-pVDZ structure). [e] rms of fit (in cm^{-1}).

TABLE 3: Equilibrium Geometries (Bond Lengths in Picometers and Angles in Degrees) of the Ground and Excited Electronic States of HSiNC

parameter	state	MP2[a]	B3LYP[a]	SAC−CI[b]	observed[c]
r(H−Si)	$\tilde{X}^1A'$	151.2	152.4	152.1	152.61(3)
r(Si−N)	$\tilde{X}^1A'$	177.8	176.8	180.0	176.3(7)
r(N−C)	$\tilde{X}^1A'$	119.0	117.8	118.6	117.0
∠(H−Si−N)	$\tilde{X}^1A'$	93.2	93.7	93.6	92.90(2)
∠(Si−N−C)	$\tilde{X}^1A'$	170.9	169.9	170.1	169.31(5)
r(H−Si)	$\tilde{A}^1A''$	147.9	149.7	149.7	
r(Si−N)	$\tilde{A}^1A''$	173.5	171.9	173.1	
r(N−C)	$\tilde{A}^1A''$	118.7	118.3	119.2	
∠(H−Si−N)	$\tilde{A}^1A''$	116.2	115.2	115.1	
∠(Si−N−C)	$\tilde{A}^1A''$	172.9	173.5	175.1	

[a] This work. Calculated using the aug-cc-pVTZ basis set. [b] This work. Calculated using the aug-cc-pVDZ basis set. [c] Ref 8.

The resulting spectroscopic constants for the ground state are given in Table 1 together with the constants (for both HSiCN and HSiNC) obtained from ab initio calculations and the previous microwave study. It can be clearly seen in Table 1 that the observed 0_0^0 band belongs to HSiNC and not HSiCN. Table 2 gives the excited state constants obtained from this work as well as the ab initio determined constants. Additional analysis using ground state combination differences confirm the spectral carrier as HSiNC. The structure of HSiNC in both its ground and $\tilde{A}^1A''$ electronic states can be found in Table 3.

Table 2 also shows some discrepancy in the estimation of the transition energy of the $\tilde{A}^1A''-\tilde{X}^1A'$ transition for HSiNC. The MP2 calculation is significantly different from the observed value. To check this discrepancy similar calculations on HSiF and HSiCl were carried out, and they also showed a significant difference between the observed and calculated values ($\sim$4000 cm^{-1} difference). To improve the estimation of the transition energy, further calculations were carried out using the symmetry-adapted cluster-configuration interaction (SAC−CI) methods of Nakatsuji et al. utilizing the aug-cc-pVDZ basis set to optimise the geometries. Once this was complete, further single point calculations were run using the larger aug-cc-pVTZ basis set. This was necessary as optimization of the full structures using the larger basis set was deemed too computationally demanding. The results of these calculations are shown in Table 2. The SAC−CI calculation gives a good estimation of the transition energy of HSiNC. To check the reliability of the result, similar calculations were carried out on HSiF and HSiCl and these gave differences of only 130 cm^{-1} and 240 cm^{-1} from the observed

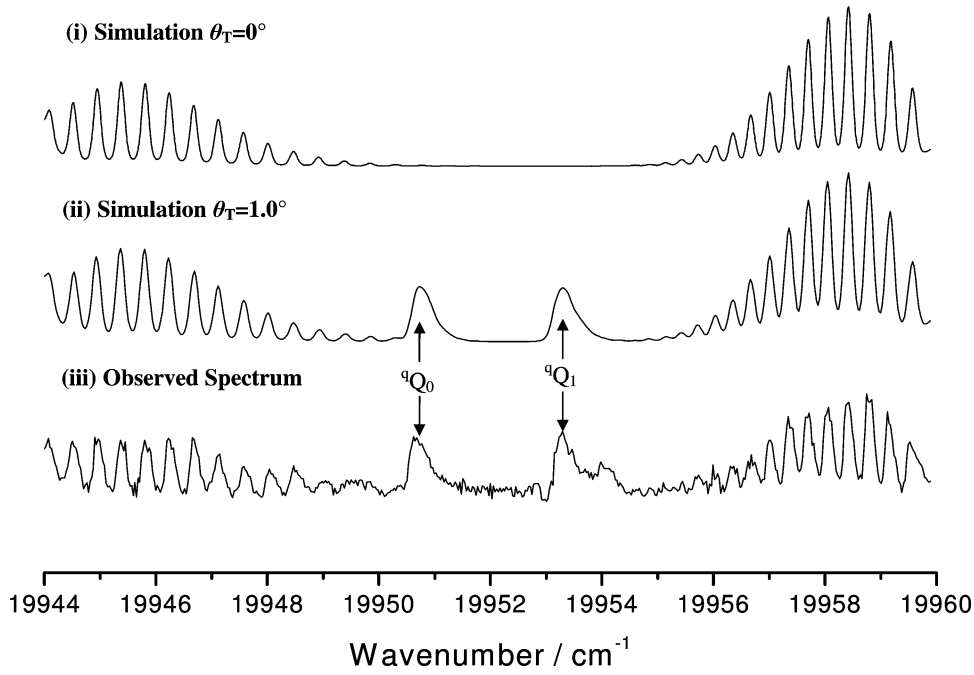

Figure 2. An expanded view of one of the regions with axis-rotation peaks. Section (i) shows the simulated spectrum with $\theta_T = 0°$; section (ii) shows the simulated spectrum with $\theta_T = 1.0°$; section (iii) shows the observed spectrum.

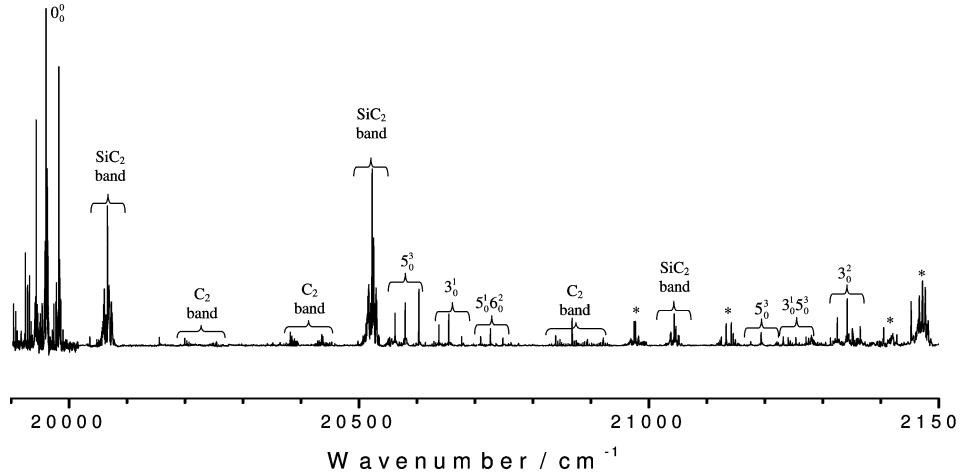

Figure 3. A portion of the low resolution spectrum of HSiNC showing the vibrational assignments. Peaks from SiC_2 and C_2 are also indicated. The peaks marked with asterisks are due to unknown contaminants.

TABLE 4: Vibrational Assignments and Wavenumber Values for the Excited ($\tilde{A}^1A''$) State Vibrational Modes of HSiNC Calculated at Different Levels of Theory Using the aug-cc-pVTZ Basis Set with All Values Given in cm^{-1}

vibrational mode (symmetry)	assignment	MP2[a] (harmonic)	MP2[a] (anharmonic)	B3LYP[a]	QCISD[a]
ν_1 (a′)	Si−H stretch	2234.1	2135.7	2065.6	2199.2
ν_2 (a′)	N−C stretch	2172.9	2216.3	2022.1	2076.5
ν_3 (a′)	Si−H wag	700.6	689.3	656.0	707.0
ν_4 (a′)	Si−N stretch	669.0	662.0	685.9	676.4
ν_5 (a′)	Si−N−C in-plane bend	200.4	211.8	203.3	187.1
ν_6 (a″)	Si−N−C out-of-plane bend	234.3	246.2	268.6	240.9

[a] This work. Unscaled wavenumbers.

values, showing that the transition energies estimated using SAC−CI are consistently closer to the observed values.

Axis-Rotation

One of the most interesting features of this spectrum is the occurrence of axis-rotation peaks. Originally this phenomenon was discussed by Hougen and Watson.[2] When there is a geometry change on electronic excitation, the inertial axes of the ground and excited states do not coincide. This is due to the molecule fixed axis system for each state as defined by the Eckart conditions. These conditions allow, to a large extent, separation of the rotational motion from the internal vibrational motions. Although the coupling between these motions cannot be completely separated, the Eckart conditions minimize the energy between them.[2,26] When a molecule undergoes an optical transition to a different electronic state, the definition of the

TABLE 5: Band Assignments, Band Origins, the Offset from the 0_0^0 Band, MP2 Anharmonic Values, and Approximate $(A - \bar{B})'$ Values for Each of the Observed Vibrational Bands in the LIF Spectrum of HSiNC in the $\tilde{A}^1A''$ State (All Values in cm^{-1})

assignment[a] (symmetry)	band origin[b]	offset from 0_0^0 band	ab initio prediction[c]	$(A - \bar{B})'$
0_0^0 (a′)	19950.5623	0.00		9.8087
5_0^3 (a′)	20569.746	619.16	627.6	10.282
3_0^1 (a′)	20645.225	694.65	689.3	9.816
$5_0^1 6_0^2$ (a′)	20717.18	766.70	758.0	9.594
5_0^5 (a′)	21183.051	1232.49	1248.3	10.841
$3_0^1 5_0^3$ (a′)	21260.9271	1310.35[d]	1298.6	10.294
4_0^2 (a′)			1320.3	
3_0^2 (a′)	21332.701	1382.13	1374.8	9.873
$1_0^1 6_0^1$ (a″)	22331.372	2380.77[d]	2382.3	10.303
$3_0^2 6_0^4$ (a′)			2381.5	
$4_0^2 5_0^5$ (a′)			2383.4	
$3_0^2 5_0^5$ (a′)	22357.189	2406.58	2409.9	10.404
$2_0^1 5_0^1$ (a′)	22384.623	2434.00	2429.0	10.314
$2_0^1 6_0^3$ (a″)	22871.592	2920.99[d]	2928.6	10.591
$2_0^1 5_0^2 6_0^1$ (a″)			2926.9	
$2_0^1 3_0^1$ (a′)			2902.5	

[a] Assignments are based on the ab initio results. [b] Numbers in parentheses are 1σ uncertainties in units of the last significant digit. [c] This work. Values predicted from the anharmonic MP2 calculation. [d] More than one assignment possible.

body fixed axis system switches abruptly, hence the axis-switching, axis-reorientation, or axis-rotation. The calculation of the axis-rotation parameters requires a common frame for both states, and this is achieved by application of a rotation transformation matrix. This transformation has the effect of mixing the rotational wave functions with K differing by one unit and causes the observation of "forbidden" sub-bands as well as a decrease in the intensity of lines in the main sub-bands.

There are two categories of molecular transitions which may occur as a result of axis-rotation. These are nonlinear to nonlinear transitions and linear to nonlinear transitions. Further to this, these transitions may be divided into two subcategories with the molecular system adopting a planar or nonplanar geometry in either of the states under consideration. For linear to nonlinear transitions the planar-to-planar geometry is always observed, while for nonlinear to nonlinear transitions either planar-to-planar or planar-to-nonplanar geometries may occur.

Previous examples of molecular species exhibiting axis-rotation of the linear to nonlinear type are HCO, HCN, HND, and acetylene (C_2H_2).[27−29] Previous examples of species exhibiting the most common nonlinear to nonlinear (planar-to-planar) type axis rotation are HNF,[30] HSiF,[6,7] HSiCl,[1,4] HSiBr,[1,3] HSiI,[5] HCF,[29] HCCl,[31] HCBr,[32] and HNO.[29] A number of larger systems also exhibit planar-to-planar type axis-rotation including, indole, indazole, and benzimidazole.[33] Finally, there is one example of the far less common case of nonlinear to nonlinear (planar-to-nonplanar) type axis-rotation which is thiosphosgene (Cl_2CS).[34]

The assignment of the axis-rotation peaks was very difficult in the spectrum of the 0_0^0 band of HSiNC, as the intensity of the axis-rotation peaks is comparable to those of the various contamination peaks observed in the spectrum. There is not enough data for accurate determination of the equilibrium geometries for the two electronic states; therefore, it was only possible to determine an estimate of the axis-rotation angle (θ_T). First, to unambiguously assign these peaks, it was necessary to simulate the spectrum with the inclusion of the axis-rotation peaks and compare this simulation to the experimentally observed spectrum. This was done using the Jet Beam 95 (JB95) spectral fitting program.[35] The simulation was produced by using the rotational constants obtained from the fit of the medium resolution spectrum of the 0_0^0 band and adjusting the axis-rotation angle until there was good agreement between the experimental and simulated spectra. Unfortunately one of the contaminants occurs in exactly the same region as the ${}^qQ_0$ (19950.65 cm^{-1}) and ${}^qQ_1$ (19953.27 cm^{-1}) axis-rotation peaks; therefore, estimation of θ_T was taken from the ${}^sQ_0$ (19989.75 cm^{-1}) axis-rotation peak. This iterative approach gave a "best" estimated value of $\theta_T = 1.0° \pm 0.2°$.

Figures 2 shows the observed and simulated spectrum of the ${}^qQ_0$ and ${}^qQ_1$ axis-rotation peaks. As can be seen there is very good agreement, in terms of both intensity and position of the axis-rotation peaks, between the simulated and experimental spectra. To show that the observed peaks were from an axis-rotation process, a simulation with $\theta_T = 0°$ is also included. Figure 2 also shows the problem with overlap between the assigned axis-rotation peak at ∼19953.2 cm^{-1} and some unknown contaminant in the LIF spectrum.

To get another estimate of the axis-rotation angle, a combination of the ab initio data together with the structural data from the microwave study was used.[36] The ab initio data suggests that on electronic excitation from the ground state to the first excited ($\tilde{A}^1A''$) state there is a significant change in the H−Si−N angle from approximately 93° to 116° (see Table 3). It is thought that this change in the H−Si−N angle is responsible for the appearance of the axis-rotation peaks. Following the procedure described in the paper by Hougen and Watson,[2] it is possible to determine the axis-rotation angle from the calculated equilibrium geometries of the two electronic states and to compare it against the experimentally determined value of $1.0° \pm 0.2°$. By application of the Hougen and Watson method directly to the tetra-atom HSiNC system the axis-rotation angle is predicted to be 0.81°, which is in reasonable agreement with $1.0° \pm 0.2°$ estimated from the spectrum.

Vibrational Analysis

The band system observed between 520 and 420 nm is assigned to the $\tilde{A}^1A''-\tilde{X}^1A'$ electronic transition of HSiNC. This transition corresponds to the promotion of an electron from an H−Si molecular orbital to an unoccupied out-of-plane p orbital located on the silicon atom. The LIF spectrum of HSiNC was recorded over the 19950−25000 cm^{-1} region. A section of the observed LIF spectrum is shown in Figure 3. The HSiNC spectrum consists of an intense origin band at ∼19950 cm^{-1}, with a number of additional vibrational bands at ∼20570, 20645, 20717, 21183, 21260, 21333, 22331, 22357, 22385, and 22872 cm^{-1}. The spectrum is quite complicated as there are many spectral features from other molecular species present. Many of these spectral features can be attributed to the SiC_2 band system which starts at ∼20075 cm^{-1} and from the Swann band system of C_2.[37,38] In some cases, these bands overlap with those of the HSiNC bands making assignments difficult. Also, apart from the 0_0^0 band, the intensities of the observed vibrational bands of HSiNC are weak relative those of the various contaminants.

In total, 11 vibrational bands of the HSiNC species have been tentatively assigned. Each of the observed vibrational bands was fitted using the spectral fitting program PGOPHER.[39] For each band, a rough fit was first obtained by fitting the Q-branches and floating the transition frequency value (T_0) only. Once the rough fit was complete, a more accurate fit was obtained by

TABLE 6: Vibrational Assignments and Wavenumber Values for the Ground ($\tilde{X}^1A'$) State of HSiNC Calculated at Different Levels of Theory Using the aug-cc-pVTZ Basis Set with All Values in cm^{-1}

vibrational mode (symmetry)	assignment	MP2[a] (harmonic)	MP2[a] (anharmonic)	B3LYP[a]	QCISD[a]	IR matrix study[b]
ν_1 (a′)	Si−H stretch	2125.9	2052.3	2029.3	2077.8	2017.8
ν_2 (a′)	N−C stretch	2037.2	2007.2	2096.6	2102.4	2039.5
ν_3 (a′)	Si−H wag	882.9	867.2	868.1	879.8	867.9
ν_4 (a′)	Si−N stretch	624.4	620.8	626.4	635.6	622.0
ν_5 (a′)	Si−N−C in-plane bend	204.7	208.7	219.9	205.4	
ν_6 (a″)	Si−N−C out-of-plane bend	159.2	164.6	167.0	155.0	

[a] This work. Unscaled wavenumbers. [b] Ref 12.

adding in any rotational lines which were sufficiently resolved from the low resolution fits, and the excited state rotational constants A and $\bar{B}$ were floated together with the transition frequency. In all cases the ground state parameters were fixed to those obtained from the medium resolution fit of the 0_0^0 band (see Table 1). The $(A - \bar{B})'$ values can be useful to consider in making assignments, as values which are significant different from that of the 0_0^0 band may indicate that at least one quanta of a bending mode may be present.

To aid in the assignment of the observed bands harmonic vibrational frequencies were evaluated at different levels of theory (see Table 4). For the MP2 calculations anharmonic frequencies were also evaluated. HSiNC is a bent molecule of C_s symmetry with five a′ vibrational modes labeled ν_1 (Si−H stretch), ν_2 (N−C stretch), ν_3 (Si−H wag), ν_4 (Si−N stretch), and ν_5 (Si−N−C in-plane bend), as well as one a″ vibrational mode labeled ν_6 (Si−N−C out-of-plane bend).

The assignments, band origins, offset from the 0_0^0 band, MP2 anharmonic frequencies, and approximate values of $(A - \bar{B})'$ for each band are given in Table 5. For the bands observed at 21260.92, 22331.36, and 22871.61 cm^{-1}, there are two or more possible assignments and these are also given in Table 5.

Dispersed Fluorescence Spectra

In the previous work carried out on the halosilylenes information about their ground state vibrational manifolds were obtained by carrying out emission spectroscopy. It therefore seemed prudent to attempt to carry out a similar study on HSiNC to see if similar information about the ground state may be gained. Table 6 shows the ground state harmonic frequencies calculated at different levels of theory. Again, for the MP2 calculations anharmonic frequencies were also evaluated.

Figure 4 shows the dispersed fluorescence (DF) spectrum obtained by pumping the strong $^pQ_1$ branch of the 0_0^0 band of the $\tilde{A}^1A''-\tilde{X}^1A'$ electronic transition of HSiNC. As mentioned previously the electronic transition is accompanied by a change in the H−Si−N bond angle of ≈25°, so the emission spectra are dominated by the ν_3 (Si−H wag) modes. As can be seen by the data collected, the observed progressions were very short (~3500 cm^{-1}), and no further signals were detected when the scanning range of the monochromator was extended over 10000 cm^{-1}. This corresponds to what is seen in the LIF spectra, where the entire LIF spectrum is covered between 19915 and 23500 cm^{-1}. Table 7 lists the bands observed from the DF study and their assignments.

Anharmonic Analysis

By use of the DF data given in Table 7, it is only possible to carry out an anharmonic analysis on the ν_3 vibrational mode of HSiNC. As the only observed progression in the DF spectra was for the ν_3 vibrational mode the analysis is very simple, the standard power series equation collapses down to the form given in eq 1[40]

$$G_{\nu_3} = \omega_3\nu_3 + x_{33}(\nu_3)^2 \quad (1)$$

This small amount of information still gives an indication of the accuracy of the computationally determined anharmonic values for this particular mode. The DF data given in Table 7 has been fitted to eq 1, and the results are $\omega_3 = 859.21(18)$ cm^{-1} and $x_{33} = -2.10(6)$ cm^{-1}. These values compare well with those obtained at the MP2/aug-cc-pVTZ level of theory: $\omega_3 = 867.19$ cm^{-1} and $x_{33} = -2.53$ cm^{-1}.

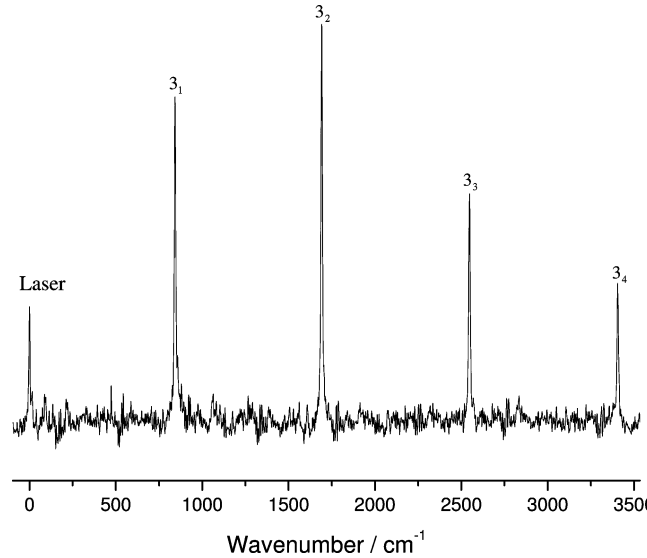

Figure 4. Dispersed fluorescence spectrum obtained by pumping the $^pQ_1$ branch of the 0_0^0 band of HSiNC. The spectrum was recorded by averaging 2000 laser shots using a slit width of 175 μm.

TABLE 7: Assignment for Each Peak and the Position of the Peaks Relative to the Laser (in cm^{-1}) for the Dispersed Fluorescence Spectrum Obtained by Pumping the $^pQ_1$ branch of the 0_0^0 band of the $\tilde{A}^1A''-\tilde{X}^1A'$ Transition of HSiNC

assignment	peak position relative to laser
3_1	857.067
3_2	1710.010
3_3	2558.793
3_4	3403.226

HSiCN

Previous experimental and theoretical work has indicated that the most stable [H, Si, C, N] isomer is HSiCN and not HSiNC. The obvious question is why has this lower energy species not been spectroscopically observed in this study? One answer to

this question is quite simple, assuming that the accuracy of the SAC−CI calculation seen in the HSiNC case is as good for predicting the transition energy for HSiCN, then the 0_0^0 band of HSiCN would appear in a region not accessible with the equipment used in this study. The predicted transition energy is 17152 cm^{-1} (corresponding to a wavelength of 583 nm), which is too far to the red end of the visible region for the PMT used in this study. Therefore, it is predicted that the electronic spectrum of HSiCN may be observable. On the other hand, if the spectrum of HSiCN is similar to that seen for HSiNC, which would seem likely, it is feasible that during the course of searching for HSiNC, some vibrational bands of HSiCN would have been encountered; however, this was not the case. Therefore the question of whether or not the electronic spectrum of HSiCN is observable remains unanswered, and open to further study.

Conclusion

In this work we have completed the first spectroscopic study of the $\tilde{A}^1A''-\tilde{X}^1A'$ transition of the HSiNC species. Together with the microwave studies on HSiNC and HSiCN and the ab initio work carried out on these species we are confident in the assignment of the observed spectra. A number of vibrational bands have been observed in the ground state and the first $^1A''$ electronic excited state and have been tentatively assigned based on the ab initio results. Detailed rotational analysis has been carried out on the 0_0^0 band resulting in the evaluation of rotational and quartic centrifugal distortion constants, with improvements made in the accuracy of some of the ground state constants compared to the previous microwave study.

The most interesting aspect of the spectrum is the appearance of the "forbidden" transitions corresponding to $\Delta K_a = 0$ and ± 2. These peaks are known as "axis-rotation" peaks, and they arise because of the significant change in the H−Si−N angle in going form the ground state to the excited state. The determination of the axis-rotation angle has been carried out in two ways; an iterative approach based on simulation of the LIF spectrum and by the approach proposed by Hougen and Watson based on a combination of the structural data provided by the microwave study for the ground state and the high-level theoretical (SAC−CI) data for the excited state. Both methods estimate an axis-rotation angle of $\sim 1.0°$ with an estimated uncertainty of $\pm 0.2°$ indicating that the ab initio data has accurately described the geometry of the excited state, assuming the ground state data from the microwave study is also accurate.

Acknowledgment. The authors wish to thank Dennis Clouthier (University of Kentucky) for the high-voltage discharge block and the circuit diagram for the pulsed high-voltage source.

Supporting Information Available: Outputs of the least-squares fits (including the GSCD fit) and extended analysis of the observed vibrational bands. This material is available free of charge via the Internet at http://pubs.acs.org.

References and Notes

(1) Herzberg, G.; Verma, R. D. *Can. J. Phys.* **1964**, *42*, 395.
(2) Hougen, J. T.; Watson, J. K. G. *Can. J. Phys.* **1965**, *43*, 298.
(3) Harjanto, H.; Harper, W. W.; Clouthier, D. J. *J. Chem. Phys.* **1996**, *105*, 10189.
(4) Harper, W. W.; Clouthier, D. J. *J. Chem. Phys.* **1997**, *106*, 9461.
(5) Billingsley, J. *Can. J. Phys.* **1972**, *50*, 531.
(6) Lee, H. U.; Deneufville, J. P. *Chem. Phys. Lett.* **1983**, *99*, 394.
(7) Dixon, R. N.; Wright, N. G. *Chem. Phys. Lett.* **1985**, *117*, 280.
(8) Sanz, M. E.; McCarthy, M. C.; Thaddeus, P. *Astrophys. J.* **2002**, *577*, L71.
(9) Guelin, M.; Muller, S.; Cernicharo, J.; Apponi, A. J.; McCarthy, M. C.; Gottlieb, C. A.; Thaddeus, P. *Astron. Astrophys.* **2000**, *363*, L9.
(10) Flores, J. R.; Perez-Juste, I.; Carballeira, L. *Chem. Phys.* **2005**, *313*, 1.
(11) Wang, Q.; Ding, Y. H.; Sun, C. C. *Chem. Phys.* **2006**, *323*, 413.
(12) Maier, G.; Reisenauer, H. P.; Egenolf, H.; Glatthaar, J. *Eur. J. Org. Chem.* **1998**, 1307.
(13) Smith, T. C.; Li, H. Y.; Clouthier, D. J.; Kingston, C. T.; Merer, A. J. *J. Chem. Phys.* **2000**, *112*, 3662.
(14) Frisch, M. J.; Trucks, G. W.; Schlegel, H. B.; Scuseria, G. E.; Robb, M. A.; Cheeseman, J. R.; Montgomery, J., J. A.; Vreven, T.; Kudin, K. N.; Burant, J. C.; Millam, J. M.; Iyengar, S. S.; Tomasi, J.; Barone, V.; Mennucci, B.; Cossi, M.; Scalmani, G.; Rega, N.; Petersson, G. A.; Nakatsuji, H.; Hada, M.; Ehara, M.; Toyota, K.; Fukuda, R.; Hasegawa, J.; Ishida, M.; Nakajima, T.; Honda, Y.; Kitao, O.; Nakai, H.; Klene, M.; Li, X.; Knox, J. E.; Hratchian, H. P.; Cross, J. B.; Bakken, V.; Adamo, C.; Jaramillo, J.; Gomperts, R.; Stratmann, R. E.; Yazyev, O.; Austin, A. J.; Cammi, R.; Pomelli, C.; Ochterski, J. W.; Ayala, P. Y.; Morokuma, K.; Voth, G. A.; Salvador, P.; Dannenberg, J. J.; Zakrzewski, V. G.; Dapprich, S.; Daniels, A. D.; Strain, M. C.; Farkas, O.; Malick, D. K.; Rabuck, A. D.; Raghavachari, K.; Foresman, J. B.; Ortiz, J. V.; Cui, Q.; Baboul, A. G.; Clifford, S.; Cioslowski, J.; Stefanov, B. B.; Liu, G.; Liashenko, A.; Piskorz, P.; Komaromi, I.; Martin, R. L.; Fox, D. J.; Keith, T.; Al-Laham, M. A.; Peng, C. Y.; Nanayakkara, A.; Challacombe, M.; Gill, P. M. W.; Johnson, B.; Chen, W.; Wong, M. W.; Gonzalez, C.; Pople, J. A. *Gaussian 03* revision D.02; Gaussian Inc.: Wallington CT, 2004.
(15) Woon, D. E.; Dunning, T. H. *J. Chem. Phys.* **1993**, *98*, 1358.
(16) Dunning, T. H. *J. Chem. Phys.* **1989**, *90*, 1007.
(17) Kendall, R. A.; Dunning, T. H.; Harrison, R. J. *J. Chem. Phys.* **1992**, *96*, 6796.
(18) Becke, A. D. *J. Chem. Phys.* **1993**, *98*, 5648.
(19) Møller, C.; Plesset, M. S. *Phys. Rev.* **1934**, *46*, 618.
(20) Frisch, M. J.; Head-Gordon, M.; Pople, J. A. *Chem. Phys. Lett.* **1990**, *166*, 275.
(21) Frisch, M. J.; Head-Gordon, M.; Pople, J. A. *Chem. Phys. Lett.* **1990**, *166*, 281.
(22) Pople, J. A.; Head-Gordon, M.; Raghavachari, K. *J. Chem. Phys.* **1987**, *87*, 5968.
(23) Nakatsuji, H. *Chem. Phys. Lett.* **1978**, *59*, 362.
(24) Watson, J. K. G. In *Vibrational Spectra and Structure: A Series of Advances*; Durig, J. R., Ed.; Elsevier: Amsterdam; Oxford, 1977; *Vol. 6*.
(25) Pickett, H. M. *J. Mol. Spectrosc.* **1991**, *148*, 371.
(26) Eckart, C. *Phys. Rev.* **1935**, *47*, 552.
(27) Brown, J. M.; Ramsay, D. A. *Can. J. Phys.* **1975**, *53*, 2232.
(28) Huet, T. R.; Godefroid, M.; Herman, M. *J. Mol. Spectrosc.* **1990**, *144*, 32.
(29) Ozkan, I. *J. Mol. Spectrosc.* **1990**, *139*, 147.
(30) Woodman, C. M. *J. Mol. Spectrosc.* **1970**, *33*, 311.
(31) Lin, A.; Kobayashi, K.; Yu, H. G.; Hall, G. E.; Muckerman, J. T.; Sears, T. J.; Merer, A. J. *J. Mol. Spectrosc.* **2002**, *214*, 216.
(32) Hall, G. E.; Sears, T. J.; Yu, H. G. *J. Mol. Spectrosc.* **2006**, *235*, 125.
(33) Berden, G.; Meerts, W. L.; Jalviste, E. *J. Chem. Phys.* **1995**, *103*, 9596.
(34) Fujiwara, T.; Lim, E. C.; Kodet, J.; Judge, R. H.; Moule, D. C. *J. Mol. Spectrosc.* **2005**, *232*, 331.
(35) Plusquellic, D. F. *User Guide to the Jb95 Spectral Fitting Program*, version 2.05.1; National Institute of Standards and Technology: Gaithersburg, MD, 2002.
(36) Sanz, M. E.; Thaddeus, P.; McCarthy, M. C. Private communication on the bond lengths of HSiCN and HSiNC.
(37) Butenhoff, T. J.; Rohlfing, E. A. *J. Chem. Phys.* **1991**, *95*, 1.
(38) Kini, K. S.; Savadatti, M. I. *J. Phys. B: At. Mol. Opt. Phys.* **1969**, *2*, 307.
(39) Western, C. M. *PGOPHER*, version 5.2.343; Bristol Laser Group, 2005.
(40) Wilson, E. B.; Cross, P. C.; Decius, J. C. *Molecular Vibrations: The Theory of Infrared and Raman Vibrational Spectra*; McGraw-Hill: New York, 1955.

JP902966Y